

Doppler-free three-photon spectroscopy of $3snf$ Rydberg states of Mg

R. Beigang and D. Schmidt

*Institut für Atom- und Festkörperphysik, Freie Universität Berlin, D-1000 Berlin 33,
Federal Republic of Germany*

A. Timmermann

Fakultät für Physik, Universität Bielefeld, D-4800 Bielefeld, Federal Republic of Germany

(Received 11 October 1983; revised manuscript received 19 December 1983)

High-resolution two-photon resonant three-photon spectroscopy was applied to investigate the $3snf$ Rydberg series of Mg. Hyperfine-induced level shifts were detected for the $^{1,3}F$ states of the odd isotope ^{25}Mg . From these measurements the hyperfine coupling constant a_{3s} of the $^{25}\text{Mg}^+$ -ion ground state was derived.

I. INTRODUCTION

Doppler-free two-photon spectroscopy with cw dye-laser radiation is a well-established technique to investigate Rydberg states with high resolution. Since there are no tunable single-mode cw dye lasers available in the uv, the energy range covered by this excitation method is limited to about $50\,000\text{ cm}^{-1}$. For higher excitation energies pulsed dye lasers were used, allowing only moderate resolution. In particular two-photon resonant three-photon spectroscopy was applied for the investigation of Ca Rydberg states.¹ Recently, it was shown that this technique can be made Doppler free and thus a high resolution can be obtained.² While in two-photon spectroscopy initial and final states have the same parity, a three-photon process combines states with opposite parity. Using Doppler-free three-photon spectroscopy, we have investigated the $3snp, 3snf$ Rydberg series of Mg starting from the $3s^2\ ^1S_0$ ground state. The excitation energy of $60\,000\text{ cm}^{-1}$ corresponds to a one-photon transition with vacuum-ultraviolet wavelength.

Laser spectroscopy of Rydberg states can yield a lot of information on the electronic structure of highly excited atoms. Measurements of term energies or lifetimes of Rydberg atoms serve as a test of wave functions. For instance, analyzing the Rydberg series by means of multichannel quantum-defect methods (MQDT) admixtures of perturbing configurations as well as singlet-triplet mixing of states can be obtained.^{3,4} However, only admixtures of the order of 1% can be deduced from MQDT analysis. The hyperfine structure is a much more sensitive test for wave functions, and admixtures of less than 10^{-3} can be accurately detected.⁵ Moreover, it is possible to derive the relative sign of the amplitudes of the admixed wave functions.⁶ Hyperfine-induced singlet-triplet mixing was already observed by Schüller and Jones in Hg.⁷ It gives rise to significant modifications of hyperfine structures and isotope shifts. This was demonstrated in the case of ^3He for $ns\ ^3S$ ($n=4-6$) and $nd\ ^3D$ ($n=3-6$) levels.^{8,9} Recently the influence of hyperfine interactions was studied systematically in the two-electron systems He,¹⁰ Yb,^{11,12} and the alkaline-earth elements Ca,¹³ Sr,¹³

and Ba.¹³⁻¹⁵ In this paper we report on hyperfine-induced level shifts of the $3snf$ Rydberg series of ^{25}Mg . Similar to Yb (Ref. 11) the level shifts in ^{25}Mg can directly be exploited to derive the ground-state splitting of the $^{25}\text{Mg}^+\ ^2S_{1/2}$ ion.

Hyperfine-induced level shifts occur whenever the hyperfine interaction becomes comparable to the electrostatic or spin-orbit interaction. In $msnl$ Rydberg series of two-electron systems the hyperfine interaction, due to the inner ms electron, is independent on principal quantum number n , while electrostatic and spin-orbit interaction scale with $(n^*)^{-3}$. Thus, in general, level shifts can be observed at high principal quantum numbers. Approaching the dissociation limit ($n \rightarrow \infty$), the electrostatic interaction between the valence electrons vanishes and the hyperfine components turn into the ground-state splitting of the ion. Although this behavior is quite clear at the ionization limit, it is much more complicated below the ionization limit in the case of heavier alkaline-earth elements due to n mixing between adjacent series members¹⁶ and high-order effects.¹⁵

In Mg, the hyperfine-induced level shifts can be observed in the $3snf$ series already at low principal quantum numbers. The description is simplified because the separation of adjacent series members is large compared to the fine and hyperfine structure, so that n mixing can be neglected. The singlet-triplet separation of $3snf\ ^{1,3}F$ states is in the order of the hyperfine splitting for $n \sim 14$. For principal quantum numbers $n \sim 60$ the singlet-triplet separation becomes even negligible. In consequence, level shifts of the $^1F, ^3F$ terms which correspond to the hyperfine splitting of the $^{25}\text{Mg}^+$ -ion ground states can be observed.

II. EXPERIMENTAL

The experimental setup (see Fig. 1) basically consists of two frequency-stabilized ring dye lasers. In a first step, the $3s\ 3d\ ^1D_2$ state was populated from the $3s^2\ ^1S_0$ Mg ground state. For this off-resonant two-photon transition a blue dye laser ($\lambda=431.0\text{ nm}$) with an output power of 150 mW was focused into the Mg vapor. Since the experimental arrangement is Doppler limited, only atoms of a

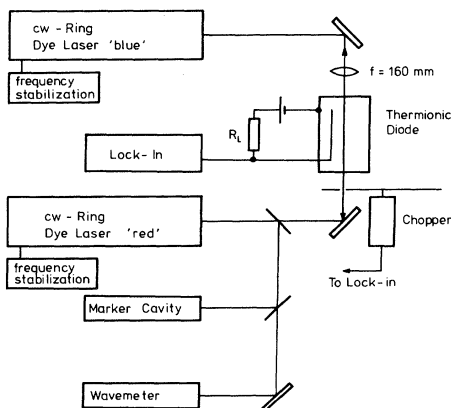


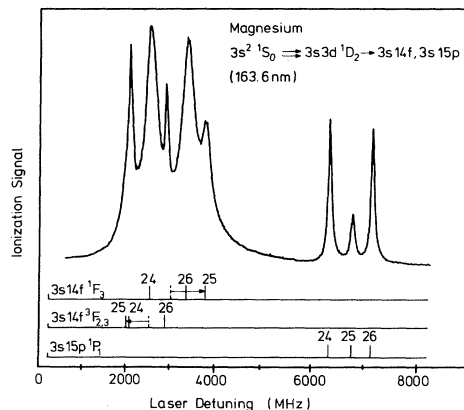
FIG. 1. Experimental setup.

selected velocity ensemble with respect to the laser-beam propagation were excited. In a second step, this velocity-selected group of atoms was then promoted to $3np, nf$ Rydberg states with a counterpropagating red dye laser. With the dye DCM (exciton) this laser was tunable up to 680 nm. The output power was reduced to 20 mW, to suppress power broadening. In order to match the excitation volume the red laser beam was tightly focused.

The Mg vapor of ~ 50 -mTorr pressure was produced in a heat-pipe oven. Approximately 200–300-mTorr Ar were added as buffer gas to prevent the cell windows from contamination. It is well known that thermionic detection is extremely sensitive for Rydberg atoms.¹⁷ We have used a thermionic ring diode as a detection device.¹⁸ Only a small fraction of ground-state atoms were excited to the low-lying intermediate $3s3d^1D_2$ state. However, since the second step is nearly saturated, they were efficiently pumped to the Rydberg states and ionized. The thermionic diode runs with a small negative bias voltage; the change in diode current was measured by means of a load resistor. Afterwards the signal was processed with conventional lock-in techniques and traced on a strip-chart recorder. By means of a confocal interferometer (free spectral range 258 MHz) frequency markers were recorded simultaneously allowing for determination of the spacing of different excitation signals.

III. RESULTS AND DISCUSSION

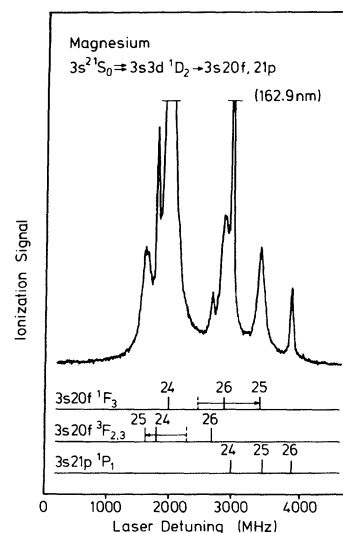
Typical examples of high-resolution three-photon excitation spectra are shown in Figs. 2 and 3. While the first laser with the frequency Ω_1 was fixed at the two-photon resonance ($3s^2^1S_0 - 3s3d^1D_2$), the second laser with the frequency Ω_2 was tuned over the resonances ($3s3d^1D_2 - 3snp, nf$). The spectra of the $3s14f, 3s15p$ states (Fig. 2) and the $3s20f, 3s21p$ states (Fig. 3) display nearly equal isotope shifts between the even isotopes ^{24}Mg and ^{26}Mg for both the 1P_1 and the $^1,^3F$ states. For the odd isotope ^{25}Mg , the 1F_3 state is considerably shifted to the high-energy side and the 3F_3 level of ^{25}Mg to the low-energy side of the spectrum. In Fig. 2 the 3F_3 signal of ^{25}Mg is masked by the ^{24}Mg 1F_3 peak. Besides the 1F_3 levels, 3F_3 states are observed for the even isotopes. This

FIG. 2. Three-photon excitation spectrum of the $3s14f, 3s15p$ configurations of Mg.

can be explained by small deviations from pure LS coupling in the intermediate as well as in the final state. Thus from the even isotopes the singlet-triplet separation $\Delta E_{ST} = E(^1F_3) - E(^3F_3)$ was determined. The values derived from both isotopes ^{24}Mg and ^{26}Mg are listed in the last column of Table I. In Fig. 4, ΔE_{ST} is plotted versus the principal number n . ΔE_{ST} is expected to depend on the effective quantum number $n^* = n - \delta$ (δ is the quantum defect) by

$$\Delta E_{ST} = C(n^*)^{-3}. \quad (1)$$

The solid line in Fig. 4 represents the $(n^*)^{-3}$ law with the constant $C = 1.475 \times 10^6$ MHz and $\delta = 0.04$. Since the singlet-triplet separation could only be resolved up to $n = 29$, ΔE_{ST} was extrapolated for higher principal quantum numbers (see Table I). A regular term sequence of the 1F_3 and 3F_3 levels was observed for the principal quantum numbers under investigation ($n \geq 14$). It should be noted, however, that for $n = 4, 5$, and 6 singlet states are inverted.¹⁹ Consequently, a crossing must occur for

FIG. 3. Three-photon excitation spectrum of the $3s20f, 3s21p$ configurations of Mg.

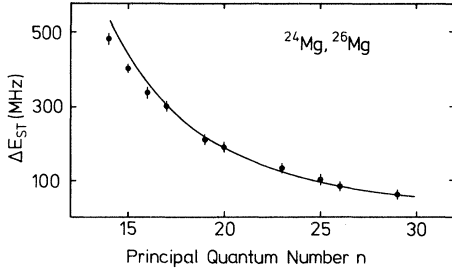


FIG. 4. Measured and calculated (solid line) singlet-triplet separation ΔE_{ST} vs principal quantum number n .

intermediate quantum numbers. This might be indicated by the small deviation of the measured singlet-triplet separation from the calculated values (solid curve in Fig. 4) for low principal quantum numbers n . By extending our work to lower principal quantum numbers we intend to measure the fine-structure trend of the $3snf$ series.

Since the two-photon resonant three-photon spectroscopy is a velocity selective excitation method, different groups of isotopes are populated. For that reason the intensities do not correspond to the natural abundance of the isotopes (^{24}Mg , 79%; ^{25}Mg , 10%; ^{26}Mg , 11%). This can be used to advantage because tuning of the first two-photon step permits a clear identification of the excitation signals with respect to the isotopes. On the other hand, the resonance frequencies for the second laser step are velocity tuned also. Considering different isotopes the frequency differences of the second laser $\delta\Omega_2$ are not the frequency differences for atoms at rest. Information of intermediate and final states can be obtained by recording spectra with co- and counterpropagating laser beams.^{20–22,2} Since the isotope shifts and hyperfine structures of the first transition $3s^2^1S_0 - 3s3d^1D_2$ have al-

ready been measured with high accuracy,²³ we restrict the experiments to the second transition $3s3d^1D_2 - 3snf, nf$ by using counterpropagating laser beams. From the measured laser frequencies $\delta\Omega_2$ relative to the $3s3d^1D_2 - 3snf^1F_3$ transition of ^{24}Mg , the atomic line position for the different isotopes is calculated. For counterpropagating laser beams the relation is given by

$$\delta\Omega_2(i,j) = \delta\omega_2(i,j) + \frac{\omega_2}{\omega_1} \delta\omega_1(i,j). \quad (2)$$

$\delta\Omega_2(i,j) = \Omega_2(i) - \Omega_2(j)$ is the detuning of the second laser with respect to the isotopes (i) and (j). $\delta\omega_1(i,j) = \omega_1(i) - \omega_1(j)$ and $\delta\omega_2(i,j) = \omega_2(i) - \omega_2(j)$ are the shifts for the first and second transition for atoms at rest. In principle, for the odd isotope ^{25}Mg the hyperfine structure of the intermediate state has to be taken into account. However, in the case of the $3s3d^1D_2$ level the hyperfine splitting is only a few megahertz²³ and can be neglected for these investigations. In Table I the measured shifts given in laser frequency $\delta\Omega_2$, with respect to the 1F_3 level of ^{24}Mg and the corresponding frequency shifts for atoms at rest $\delta(\omega_1 + \omega_2)$, are summarized in the first three columns.

In the following we will discuss the hyperfine-induced level shifts of $3snf^1,3F$ Rydberg states of ^{25}Mg and the determination of the Fermi-contact term a_{3s} from these data. The measured level shifts of 1,3F states of ^{25}Mg versus principal quantum number n are plotted in Fig. 5. For the unperturbed line position a value $\delta(\omega_1 + \omega_2) = 1840$ MHz relative to the 1,3F state of ^{24}Mg was chosen. In doing so we assume that the ratio of the isotope shift in the $3s^2^1S_0 - 3snf^1,3F$ transition corresponds to the shift in the $3s^2^1S_0 - 3snd^1D_2$ transition $\delta\omega_1(24,26)/\delta\omega_1(25,26) = 1.91$,²³ which is the ratio of the normal mass shifts. As can be seen in Fig. 5 the level shifts for the

TABLE I. All frequencies are measured in MHz.

Mg $3snf$	$^{25}\text{Mg}(^1F_3) - ^{24}\text{Mg}(^1F_3)$		$^{25}\text{Mg}(^3F) - ^{24}\text{Mg}(^1F_3)$		$^{26}\text{Mg}(^1F_3) - ^{24}\text{Mg}(^1F_3)$		$^{24}\text{Mg}, ^{26}\text{Mg}$ $E(^1F_3) - E(^3F_3)$
	$\delta\Omega_2$	$\delta(\omega_1 + \omega_2)$	$\delta\Omega_2$	$\delta(\omega_1 + \omega_2)$	$\delta\Omega_2$	$\delta(\omega_1 + \omega_2)$	
14	1242	2641			829	3504	479
15	1268	2664			838	3507	402
16	1335	2728			855	3519	337
17	1333	2724	-394	997	850	3510	300
19	1382	2770	-374	1014	853	3506	211
20	1397	2783	-366	1020	869	3520	189
23	1460	2843	-341	1042	886	3531	133
25	1455	2837	-319	1063	876	3518	99
26	1465	2846	-316	1065	887	3528	82
29	1482	2862	-318	1062	881	3520	60
30	1486	2866	-298	1082	889	3529	55 ^a
33	1483	2862	-302	1077	890	3526	41
34	1480	2858	-305	1073	878	3513	38
39	1514	2891	-297	1080	897	3531	25
40	1504	2881	-289	1088	890	3523	23
42	1480	2857	-314	1063	869	3502	20
53	1513	2889	-288	1088	895	3526	10
62	1510	2885	-278	1098	893	3523	6
84	1501	2876	-257	1118	885	3515	2

^aFor $n > 29$, the singlet-triplet separation was extrapolated using Eq. (1) (see text).

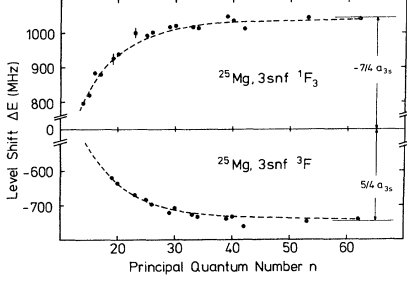


FIG. 5. Level shifts of the $3snf$ $1,3F$ Rydberg series of ^{25}Mg . Comparison between calculated energy shift (dashed line, $F = \frac{7}{2}$) and experimental data (points).

$3snf$ $1,3F$ states are increasing, going from lower to higher principal quantum numbers n . Approximately for $n \geq 45$ the level shifts remain constant, matching the hyperfine splitting of the $^{25}\text{Mg}^+$ ($I = \frac{5}{2}$)-ion ground state, as demonstrated in Fig. 6. In the ionization limit the nf $1F_3$ levels turn into the upper $F=2$ component, the nf $3F$ series proceeds to the lower $F=3$ component.

The observed shifts of the $3snf$ series of ^{25}Mg can be described, taking into account only the singlet-triplet separation. The calculations are based on the Hamiltonian

$$\mathcal{H}_1 = \frac{e^2}{r_{12}} + a_{3s} \vec{I} \cdot \vec{s} . \quad (3)$$

The first and the second part represent the electrostatic interaction and the hyperfine interaction of the $3s$ electron, respectively. The electrostatic interaction causes the splitting into singlet and triplet terms; spin-orbit effects are omitted. That is, the LS -coupling scheme is a good approximation in Mg and the $3F_{2,3,4}$ states are supposed to be nearly degenerate. Considering the hyperfine interaction, only the Fermi-contact term of the inner $3s$ electron is important. For high-Rydberg states effects of the outer nl electron can be neglected. Since $\vec{F} = \vec{I} + \vec{J}$ is a good quantum number, the wave functions of the $3snf$ configuration can be expressed as a superposition of unperturbed singlet and triplet states

$$|\Psi\rangle_F = \alpha |\Psi(1F_3)^0\rangle_F + \beta |\Psi(3F_4)^0\rangle_F + \gamma |\Psi(3F_3)^0\rangle_F + \delta |\Psi(3F_2)^0\rangle_F . \quad (4)$$

Diagonalization of the Hamiltonian [Eq. (3)] results in the perturbed level energies \tilde{E} and the mixing coefficients $\alpha, \beta, \gamma, \delta$. The singlet-triplet separation was measured for principal quantum numbers up to $n=29$. For higher n the extrapolated values using Eq. (1) were taken (see Table I). From the four possible wave functions $|\Psi\rangle_F$ for each F value two have considerable $|\Psi(1F_3)^0\rangle$ contributions α . Since the transition moment depends on the singlet admixture, only two excited states $|\Psi\rangle_F$ can be observed. The dashed curve in Fig. 5 is the result of calculations for

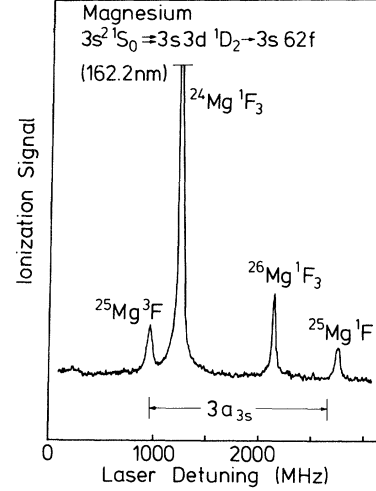


FIG. 6. Three-photon excitation spectrum of the $3s$ $62f$ configuration of Mg. The hyperfine splitting $3a_{3s}$ of the $^{25}\text{Mg}^+$ ion is indicated.

the $F = \frac{7}{2}$ component. The a_{3s} hyperfine coupling constant was varied to fit the experimental data. It should be noted that the spacing to adjacent F components is too small to be resolved in the spectra, e.g., for $n=14$ the total splitting is $E(F = \frac{1}{2}) - E(F = \frac{11}{2}) \sim 18$ MHz. This splitting decreases with increasing n .

The fit procedure yields a value of $a_{3s} = -596(2)$ MHz and is in agreement with $a_{3s} = -596.254\,376(54)$ MHz obtained by laser optical pumping double-resonance techniques.²⁴ Although the accuracy of our measurement is not as high as in Ref. 24, the determination of hyperfine splittings of ground-state ions by means of Rydberg state spectroscopy in neutral atoms might be an alternative if transitions from the ion ground state are not practical with laser sources. The accuracy can be considerably improved applying a frequency-offset locking technique, which allows for an accuracy of 100 kHz.²⁵

As already mentioned above, besides the $3snf$ series the $3snp$ $1P_1$ series of all stable Mg isotopes were observed (see Figs. 2 and 3). For the odd isotope ^{25}Mg a hyperfine-induced level shift is again observed. The $3s4p$ $1P_1$ state, for instance, is shifted approximately 130 MHz to the high-energy side. However, compared to the $3snf$ series the shifts are smaller due to the fact that the electrostatic interaction still exceeds the hyperfine interaction. An evaluation of the shifts in the $3snp$ $1P_1$ series was not carried out, because the energy levels of the $3P$ states and the spin-orbit splittings are unknown.

Furthermore, the spectra yield directly to the energy separation between the $3snp$ $1P_1$ and $3s(n-1)f$ $1F_3$ states for even isotopes. Since the level energies of the $3snp$ $1P_1$ are available,¹⁹ absolute level energies for the $3snf$ $1F$ series can be determined in principle. In Table II, however, we have restricted ourselves to the energy differences of the $3s(n-1)f$ $1F_3$ states relative to the $3snp$ $1P_1$ levels, because these values are by far more accurate than the absolute level energies of the $3snp$ $1P_1$ series given in Ref. 19.

TABLE II. Level energies of the $3s(n-1)f^1F_3$ states relative to the $3snf^1P_1$ states of Mg.

$3snf$	E (cm ⁻¹) ^a	$3snf^1P_1 - 3s(n-1)f^1F_3$ E (cm ⁻¹)
15	61 107.34	0.1266
16	61 108.24	0.0963
17	61 239.83	
18	61 289.19	0.0591
20	61 365.55	0.0392
21	61 395.43	0.0324
24	61 462.82	0.0196
26	61 494.90	0.0149
27	61 508.24	0.0128
30	61 540.26	0.0089
31	61 548.81	0.0080
34	61 570.11	
35	61 575.99	0.0067
40	61 598.87	0.0041
41	61 602.44	0.0031

^aEnergies are taken from Ref. 19.

IV. CONCLUSION

In summary we have shown that with two-photon resonant three-photon excitation high-resolution spectroscopy can be performed in an energy range of more than 60 000 cm⁻¹. The singlet-triplet separation in the $3snf$ series could be resolved, confirming a regular term order for principal quantum numbers $n > 14$. From the study of the hyperfine-induced level shift of the $3snf$ Rydberg series in ²⁵Mg the hyperfine coupling constant of the ²⁵Mg⁺-ion ground state was derived. This method should be applicable in principle also for other two-electron atoms if suitable Rydberg series with high angular momenta l are chosen, where the hyperfine splitting exceeds the fine-structure separation already at low principal quantum numbers n .

ACKNOWLEDGMENTS

We thankfully acknowledge helpful discussions with Professor Dr. E. Matthias and Dr. P. J. West and the continuous support of Professor Dr. R. Wallenstein. This work was supported by the Deutsche Forschungsgemeinschaft, Sonderforschungsbereich 161.

- ¹R. Beigang and J. J. Wynne, *Opt. Lett.* **6**, 295 (1981).
²U. Majewski, H. Rinneberg, and J. Neukammer, *Phys. Rev. Lett.* **51**, 1340 (1983).
³W. Hogervorst, *Comments At. Mol. Phys.* **13**, 69 (1983).
⁴W. E. Cooke, *Atomic Physics 7*, edited by D. Kleppner and M. F. Pipkin (Plenum, New York, 1981), p. 167.
⁵R. Beigang, K. Lücke, and A. Timmermann, *Phys. Rev. A* **27**, 587 (1983).
⁶H. Rinneberg and J. Neukammer, *Phys. Rev. Lett.* **49**, 124 (1982).
⁷H. Schüler and E. G. Jones, *Z. Phys.* **77**, 801 (1932).
⁸P. F. Liao, R. R. Freeman, R. Panock, and L. M. Humphrey, *Opt. Commun.* **34**, 195 (1980).
⁹F. Biraben, E. De Clerq, E. Giacobino, and G. Grynberg, *J. Phys. B* **13**, L685 (1980).
¹⁰L. A. Bloomfield, H. Gerhardt, and T. W. Hänsch, *J. Phys. B* **16**, L89 (1983).
¹¹L. Barbier and R.-J. Champeau, *J. Phys. (Paris)* **41**, 947 (1982).
¹²U. Majewski, H. Rinneberg, and J. Neukammer (to be published).
¹³R. Beigang and A. Timmermann, *Phys. Rev. A* **25**, 1496 (1982).
¹⁴H. Rinneberg, J. Neukammer, and E. Matthias, *Z. Phys.* **A306**, 11 (1982); H. Rinneberg and J. Neukammer, *Phys. Rev. Lett.* **49**, 124 (1982); *Phys. Rev. A* **27**, 1779 (1983).
¹⁵E. R. Eliel and W. Hogervorst, *Phys. Rev. A* **27**, 2995 (1983); *J. Phys. B* **16**, 1881 (1983).
¹⁶R. Beigang, W. Makat, A. Timmermann, and P. J. West, *Phys. Rev. Lett.* **2**, 771 (1983).
¹⁷D. Popescu, I. Popescu, C. Ghita, and O. Zamfir, *Br. J. Appl. Phys.* **15**, 1171 (1964).
¹⁸R. Beigang, W. Makat, and A. Timmermann, *Opt. Commun.* **43**, 253 (1984).
¹⁹W. C. Martin and R. Zalubas, *J. Phys. Chem. Ref. Data* **9**, 1 (1980).
²⁰C. Delsart and J.-C. Keller, *Opt. Commun.* **15**, 91 (1975).
²¹J. E. Bjorkholm and P. F. Liao, *Phys. Rev. A* **14**, 751 (1976).
²²P. F. Liao and J. E. Bjorkholm, *Phys. Rev. Lett.* **36**, 1543 (1976).
²³R. Beigang and A. Timmermann, *J. Phys. (Paris) Suppl.* **C7**, 137 (1983); R. Beigang, W. Makat, and A. Timmermann (to be published).
²⁴W. M. Itano and D. J. Wineland, *Phys. Rev. A* **24**, 1364 (1981).
²⁵H. Gerhardt, F. Jeschonnek, W. Makat, F. Schneider, A. Timmermann, R. Wenz, and P. J. West, *Appl. Phys.* **22**, 361 (1980).